THE JOURNAL OF PHYSICAL CHEMISTRY B

ARTICLE

pubs.acs.org/JPCB

Importance of Polar Solvation for Cross-Reactivity of Antibody and Its Variants with Steroids

Parimal Kar,[†,‡] Reinhard Lipowsky,[†] and Volker Knecht*[,†]

[†]Department of Theory and Bio-Systems, Max Planck Institute of Colloids and Interfaces, Am Mühlenberg 1, 14476 Potsdam, Germany

[‡]Institut für Physik und Astronomie, Universität Potsdam, Karl-Liebknecht-Strasse 24-25, 14476 Potsdam, Germany

Supporting Information

ABSTRACT: Understanding the factors determining the binding of ligands to receptors in detail is essential for rational drug design. Here, the free energies of binding of the steroids progesterone (PRG) and 5β-androstane-3,17-dione (5AD) to the Diels−Alderase antibody 1E9, as well as the Leu^{H47}Trp/Arg^{H100}Trp 1E9 double mutant (1E9dm) and the corresponding single mutants, have been estimated and decomposed using the molecular mechanics-Poisson−Boltzmann surface area (MM-PBSA) method. Also the difference in binding free energies between the PRG−1E9dm complex and the complex of PRG with the antiprogesterone antibody DB3 have been evaluated and decomposed. The steroids bind less strongly to 1E9 than to DB3, but the mutations tend to improve the steroid affinity, in quantitative agreement with experimental data. Although the complexes formed by PRG or 5AD with 1E9dm and by PRG with DB3 have similar affinity, the binding mechanisms are different. Reduced van der Waals interactions as observed for 5AD−1E9dm versus PRG−1E9dm or for PRG−1E9dm versus PRG−DB3 are energetically compensated by an increased solvation of polar groups, partly contrasting previous conclusions based on structural inspection. Our study illustrates that deducing binding mechanisms from structural models alone can be misleading. Therefore, taking into account solvation effects as in MM-PBSA calculations is essential to elucidate molecular recognition.

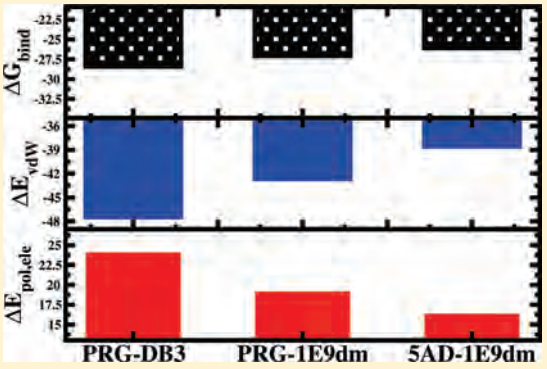

1. INTRODUCTION

The recognition of an antigen by an antibody with high affinity and specificity is an essential process of the immune response. The immune system's ability to produce antibodies against foreign antigens has been exploited to design receptors for a wide range of chemical and biochemical applications.[1] This is of particular interest in medicinal chemistry because the action of most drugs is caused by the binding of the drug to its target receptor. Hence, understanding the factors that determine the binding of ligands to receptors at the atomic level is a crucial prerequisite to successful rational drug design. In general, shape complementarity, hydrogen bonds, salt bridges, and polar interactions between the binding partners are considered important for discrimination and specificity of molecular recognition processes.[2,3]

X-ray crystallography and other biochemical methods are frequently used to characterize antibodies and provided lots of data on the structure and function of these proteins.[4−8] The structures of several steroid-binding antibodies have been determined by X-ray crystallography thus providing an atomic level understanding of steroid binding.[4,9,10] The X-ray crystallographic structure of the monoclonal antiprogesterone antibody DB3, in an unliganded form and complexed with progesterone (PRG) and several PRG-like steroids have been determined by Arevalo et al.[11,12] It has been shown that DB3 binds PRG with high affinity and cross-reacts with several progesterone-like steroids with nanomolar affinities.[12]

DB3 shares 91% sequence identity to the antibody 1E9. The antibody 1E9 was the first antibody catalyst for the Diels−Alder reaction.[13] The latter denotes the cycloaddition between tetrachlorothiophene oxide[14] and *N*-ethylmaleimide.[15] The steroid binding DB3 and the Diels−Alderase 1E9 antibodies have been derived from the same germ line sequence VGAM3.8 and Vk5.1 for the variable heavy and light chain gene segments, respectively. However, their variable domains exhibit 36 sequence differences. Six of these amino acids, namely residues H47, L89, L94, H97, H100, and H100b, are located in the combining site, providing an explanation for their different functions[16] and weak cross-reactivity.[17] However, some of the key combining site residues are identical. The residue Asn^{H35} is crucial for the ligand binding by DB3 and catalysis by 1E9, and Trp^{H50} contributes significantly to ligand binding in both cases.[12,16] Otherwise, specific interactions between the cavity-lining residues and the steroid skeleton, particularly with the D ring, are essential,[11,12] whereas, for

Received: February 16, 2011
Revised: May 4, 2011
Published: May 19, 2011

efficient catalysis by 1E9, shape complementarity combined with a few specific interactions are most important.[18,19]

Recently Piatesi et al.[20] have shown by site-directed mutagenesis and binding studies that only two mutations are required to interconvert the binding specificity of 1E9 and DB3. The

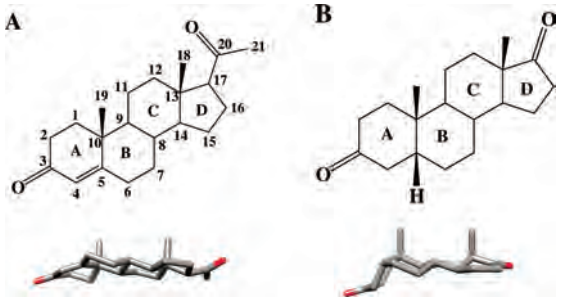

Figure 1. Chemical structure of (A) Progesterone and (B) 5β-androstane-3,17-dione. Colors distinguish between carbons or hydrocarbons (gray) and oxygen atoms (red). The figures were created with the graphics programs ChemDraw[22] and Chimera.[23]

Leu^{H47}Trp/Arg^{H100}Trp 1E9 double mutant (1E9dm) binds both steroids with nanomolar (nM) affinity and recapitulates the binding specificity of DB3 for a panel of structurally and configurationally distinct steroid molecules. Recently, the crystal structures of 1E9dm complexed with progesterone (PRG) or 5β-androstane-3,17-dione (5AD) have been determined by Verdino et al.[21] The chemical structure of the two steroids is shown in Figure 1. Their A rings assume different orientations relative to the rest of the steroid skeleton because of the substitution at carbon C5. Progesterone is C5-unsaturated (sp^2 hybridization) with an ~35° bent A ring. 5β-androstane-3,17-dione is 5β-substituted (sp^3 hybridization) and its A ring is almost perpendicular to the rest of the steroid skeleton.[21]

The crystallographic structures of the 1E9dm−PRG and 1E9−5AD complexes reveal that the principal axis of the steroid skeleton is rotated by ~40° in 1E9dm compared with DB3.[21] DB3 binds PRG in a syn and 5AD in an anti binding mode. A syn binding mode denotes the situation that the methyl positions C18 and C19 face Trp^{H50}, and C11 is oriented toward the exterior of the combining site where it is accessible to the solvent. An anti binding mode denotes the case that the methyl groups

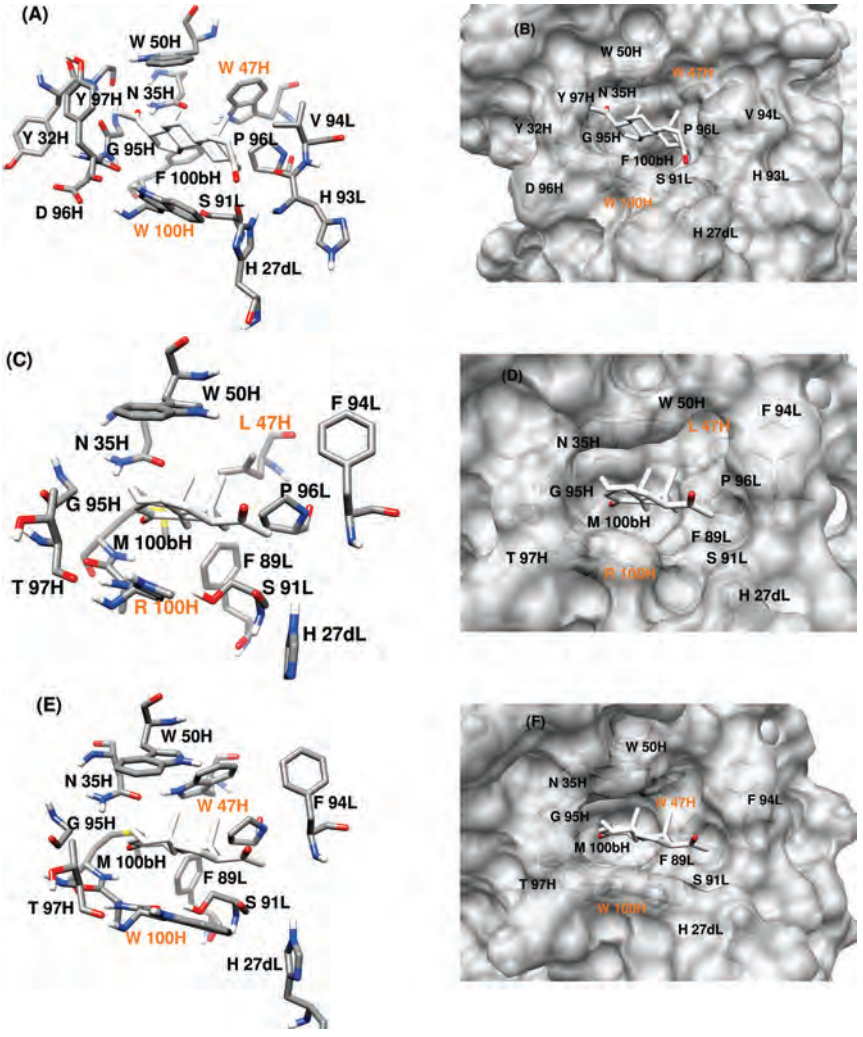

Figure 2. Structures of the binding sites of (top row) DB3, (middle row) 1E9, and (bottom row) 1E9dm with bound progesterone in stick representation with binding sites shown in (left column) stick and (right column) stick and transparent surface representation. In the left column, colors distinguish between carbons and hydrocarbons of the ligand or hydrogens of the antibodies (white), carbons of the antibodies (gray), as well as oxygen (red), and nitrogen atoms (blue). The mutated sites are indicated by orange labels. The figures were created with the software Chimera.[23]

make contacts with Trp^{H100}, whereas C11 is totally buried in the pocket.[12] However, in both modes, DB3′s specificity is considered to be exclusively based on the burial of the steroid D ring whose carbonyl group forms a hydrogen bond with Asn^{H35}. For the PRG−DB3 complex, an additional hydrogen bond is formed between the carbonyl group of the A ring and His^{L27d}. In contrast, the 1E9dm antibody binds both steroids in a syn orientation. Progesterone is bound in 1E9dm with the A ring being most deeply buried while the D ring is deeply buried in 5AD−1E9dm complex (see Figure 2). Neither the PRG−1E9dm nor the 5AD−1E9dm complex exhibit hydrogen bonds between the ligand and the protein.[21]

The differences in ligand binding of these two antibodies are caused by the discriminative space requirements of the corresponding H100b residues. In DB3, the bulky Phe^{H100b} residue in the binding site provides high shape complementarity to steroids and positions them closer to the opening of the DB3 combining site, see Figure 2A. On the other hand, 1E9dm contains the residue Met^{H100b} that reconfigures the binding pocket of the antibody 1E9dm and generates space in the base of the binding pocket. Verdino et al. argue that this allows a deeper penetration of the ligands into the binding pocket, creating more hydrophobic contacts, compensating for the lack of hydrogen bonding.[21] Indeed, 5AD forms more van der Waals contacts with 1E9dm (42) than with DB3 (20). However, in the corresponding X-ray structures PRG actually forms less contacts with 1E9dm (46) than with DB3 (59),[12,21] ruling out the mechanism proposed by Verdino et al. for PRG and calling for an alternative explanation.

More fundamentally, the view that DB3′s specificity for PRG arises mainly from the existence of two hydrogen bonds between the binding partners reflects the notion that hydrogen bonding between a protein and its ligand is a major factor of molecular recognition.[2,3] However, any hydrogen bond formed between a protein and its ligand upon binding will be accompanied with the loss of hydrogen bonds of two molecules with the solvent, and whether there is an energetic gain in the exchange of hydrogen-bonding partners depends on the relative strength of the different types of hydrogen bonds.[24] In fact, the favorable contribution of polar protein−ligand interactions appears to be typically overcompensated by an unfavorable contribution from the desolvation of polar groups. This is indicated from free energy calculations using molecular mechanics for the binding partners and a continuum description of the solvent for a range of systems including PRG−DB3.[25−27]

To elucidate the mechanisms of the cross reactivity of 1E9 and its variants with PRG and 5AD including solvent effects, we have conducted molecular dynamics simulations and free energy calculations studying the contributions arising from different molecular interactions to the binding affinities for different complexes. The complex 5AD−1E9dm, as well as the corresponding complexes of both ligands with wild type 1E9 and the single mutants were studied. The most rigorous and accurate methods to calculate binding free energies are free energy perturbation[28] and thermodynamic integration.[29] Here, the sum of small free energy changes is evaluated along a physical or alchemical multistep pathway connecting the bound and the unbound state. However, these methods are computationally very expensive. In contrast, generating conformational ensembles for the free and the bound species and evaluating the corresponding free energies using the molecular mechanics-Poisson−Boltzmann or Generalized Born surface area (MM-PB/GBSA) methods[30−32] is faster by several orders of magnitude than free energy perturbation or thermodynamic integration. The MM-PB/GBSA methods have successfully been used to estimate the binding free energy of protein−ligand[26,33] and protein−RNA[34,35] associations. This method has also been used to study the binding of steroids to DB3.[27,36] In our study, the contribution from the change in entropy of the binding partners was obtained from a normal-mode analysis (NMA)[37,38] of the complex. The results of our calculations agree well with experimental data and give insights into the origins of mutation-induced affinity changes, highlighting the importance of polar solvation for molecular recognition.

2. MATERIALS AND METHODS

2.1. Structure Generation with MD Simulations in Explicit Water. The initial coordinates for our simulations were obtained from the X-ray crystallographic structures of the 1E9dm Fab complexed with progesterone (PDB ID 2O5Y), and 5β-androstane-3,17-dione (PDB ID 2O5Z) determined to 2.05 and 2.40 Å resolution, respectively.[21] The proteins were described using the Amber ff99SB force field.[39] The ligands were assigned generalized amber force field (GAFF)[40] atom types, and AM1-BCC[41] atomic charges calculated with the antechamber[42] module of Amber.[43] The AM1-BCC charge for an atom is obtained by adding the bond charge correction (BCC) to a semiempirical quantum calculation of molecular electronic structure according to the Austin Model 1 (AM1) population atomic charge.[44] It has been shown that atomic charges obtained from this charge model emulate the HF/6-31G* (Hartree−Fock theory using a basis set 6-31G*) electrostatic potential at the surface of a molecule.[41] Backward mutations were performed manually to study the binding of steroids to (i) the wild type and (ii) single mutant variants of the antibody 1E9. The configurations were generated via simulations of the complexes in explicit water.

The complex was solvated in TIP3P[45] water using a truncated octahedron periodic box, extending at least 10 Å from the complex. Nearly 18 000 water molecules were added to solvate the complex and the resulting box size was nearly 110 Å × 110 Å × 110 Å. All bond lengths involving hydrogen atoms were constrained using the SHAKE[46] algorithm allowing the usage of a 2 fs time-step. The temperature was kept fixed at 300 K using a Langevin thermostat with a collision frequency of 2 ps^{-1}. The electrostatics were treated with the particle-mesh Ewald (PME)[47] scheme with a fourth-order B-spline interpolation and a tolerance of 10^{-5}. The nonbonded cutoff was 8 Å and the nonbonded pair list was updated every 50 fs.

The following protocol was used in our simulations: (i) the complex was first optimized by 500 steps of steepest descent followed by another 500 steps of conjugate gradient minimization, keeping all atoms of the complex restrained to their initial position with a weak harmonic potential. (ii) After the minimization, 50 ps of constant volume MD simulation with a force constant of 2 kcal·mol^{-1} Å^{-2} on the complex was performed in order to equilibrate the solvent at 300 K without undesirable drifts of the structure. (iii) Next, a 50 ps MD simulation with a force constant of 2 kcal·mol^{-1} Å^{-2} on the complex was carried out at a pressure of 1 atm to equilibrate the density using Berendsen's barostat. (iv) Then, the complex was equilibrated for 500 ps without restraint. After the equilibration phase, a 10 ns simulation at constant pressure was conducted. This corresponds to a 3- to 5-fold increase in time scale compared to current state-of-the-art simulation protocols in this field. Coordinates were

saved after every 10 ps, resulting in 1000 configurations for each simulation.

2.2. MM-PBSA Calculations. The most common receptor−ligand (R-L) association reaction is governed by the following equation

$$R + L \leftrightarrow RL \quad (1)$$

where all the reactants are assumed to be in aqueous solution. The binding affinity is determined from the free energies of the receptor (R), the ligand (L), and the complex (RL):

$$\Delta G_{bind} = G_{RL} - (G_R + G_L) \quad (2)$$

The free energy of each species (R, L, RL) is estimated from

$$G = \langle E_{MM} \rangle + \langle G_{pol} \rangle + \langle G_{np} \rangle - T\langle S_{MM} \rangle \quad (3)$$

Here, E_{MM} is the molecular mechanics gas-phase energy of the species, G_{pol} is the polar contribution to the solvation free energy of the species, estimated from the solution of the linear Poisson−Boltzmann (PB) equation ($G_{pol,PB}$), G_{np} is the nonpolar solvation free energy, estimated from the solvent accessible surface area (SASA) of the species, T is the absolute temperature of the system, and S_{MM} is the entropy of the species, calculated from a normal-mode analysis of harmonic frequencies estimated at the molecular mechanics (MM) level. The gas-phase molecular mechanics energy E_{MM} can be expressed as

$$E_{MM} = E_{cov} + E_{elec} + E_{vdW} \quad (4)$$

where E_{cov}, E_{elec}, and E_{vdW} denote the contributions from covalent, electrostatic, and van der Waals interactions, respectively. The contributions from nonpolar solvation, (G_{np}), was evaluated from[48]

$$G_{np} = \gamma A_{sasa} \quad (5)$$

where A_{sasa} is the solvent accessible surface area (SASA) and γ = 0.023 kcal·mol^{-1} Å^{-2}. The SASA was estimated using a probe radius of 1.4 Å. The averages in eq 3 are calculated from an ensemble of molecular configurations taken from a molecular dynamics simulation to capture the effects of motion. In order to mimic the in vitro binding event and to include the effects of the conformational changes upon binding, each of the three terms in eq 2 should be calculated from an individual simulation of the protein, the ligand and the complex (multitrajectories method).[49] As this scheme relies on sufficient sampling of configurational space, computational resources and time would be an issue. In practice, in order to reduce the time-consumption in simulation and to obtain stable energies, only the complex is simulated and all the three free energy terms are estimated from this single molecular dynamics trajectory.[49,50] In that case, the covalent energy (E_{cov}) as well as the intramolecular electrostatic and van der Waals energy cancel out in the calculation of ΔG_{bind}. This single trajectory method is based on the assumption that the conformational changes of the protein and ligand upon binding is negligible. Taking the structures of all the three species from a single trajectory may remove the noise resulting from sampling inconsistencies and reduce the inherent error in force field and implicit solvation energies. Earlier studies,[49,51] though, have shown that the multitrajectory and the single trajectory method yield similar trends. Verdino and co-workers[21] have found that the steroid binding with the double mutant 1E9dm does not induce conformational changes other than in the binding site. A root mean-squared deviation (rmsd) of 0.23−0.27 Å is observed for all backbone atoms. This is an order of magnitude smaller than the deviation from the experimental structure typically seen in MD simulations.

The MMPBSA.py.MPI script in Amber-11 was used to determine total molecular-mechanical energies (E_{gas}), the covalent energy (E_{cov}), as well as the van der Waals (E_{vdW}), and electrostatic (E_{elec}) components. This script performs automatically all the necessary steps to estimate the binding free energy of protein−ligand complexes using the MM-PBSA method. The electrostatic contribution to the solvation free energy (G_{PB}) was estimated by solving the linear Poisson−Boltzmann equation for each solute configuration using the Adaptive Poisson−Boltzmann Solver (APBS).[52] For this purpose, the iAPBS patch was used to call APBS from the Sander module in Amber-11. In iAPBS, the grid spacing was set to 0.5 Å in all directions and the internal and external dielectric constants were set to 1 and 80, respectively. The ionic strength was set to 0.1 M. The ratio between the longest dimension of the rectangular finite-difference grid and that of the solute was set to 4.0. The PB equation was solved using 1000 linear steps of finite difference.

The entropic contribution to the affinity of steroids for the proteins was calculated by normal-mode analysis (NMA) of the harmonic vibrational frequencies of 40 configurations considering the complete protein using the Amber *mmpbsa_py_nabnmode* program. To this aim, each configuration was energy minimized with a Generalized-Born solvent model using a maximum of 50 000 steps and a target root-mean-square (rms) gradient of 10^{-4} kcal mol^{-1} Å^{-1}.

The relative binding free energies from our simulations were compared to the corresponding experimental values, $\Delta\Delta G_{exp}$, determined from

$$\Delta\Delta G_{exp} = -k_B T \ln r_{exp} \quad (6)$$

Here k_B is the Boltzmann constant, T is the absolute temperature, and r is the relative binding constant. The relative binding constant is defined as $r \equiv K'_a/K_a$, where K'_a or K_a denote the binding constant for the mutant or wild type 1E9, respectively. The value for r_{exp} is determined from the values of these binding constants as determined experimentally. In addition, the relative binding free energies from our simulations, $\Delta\Delta G_{sim}$, were converted into a relative binding constant, r_{sim}, again using eq 6, replacing $\Delta\Delta G_{exp}$ by $\Delta\Delta G_{sim}$ as well as r_{exp} by r_{sim} and solving the equation for r_{sim}, which leads to

$$r_{sim} = \exp(-\Delta\Delta G_{sim}/k_B T) \quad (7)$$

The relative binding constant for each steroid mutant complex was evaluated in terms of a corresponding confidence intervall $[r_1,r_2]$, where r_1 and r_2 were determined from eq 7, replacing $\Delta\Delta G_{sim}$ by $\Delta\Delta G_{sim} \pm$ se($\Delta\Delta G_{sim}$) with se($\Delta\Delta G_{sim}$) denoting the standard error of the relative binding free energy.

In order to elucidate the binding mechanisms, we also provide the individual contributions to the binding free energies. Here, the contribution from the van der Waals or electrostatic interactions between the antibody and the steroid, ΔE_{elec} or ΔE_{vdW}, respectively, the polar or nonpolar solvation free energy, ΔG_{pol} or G_{np}, respectively, and the contribution from the configurational entropy of the binding partners, denoted as $-T\Delta S_{MM}$, were considered. To study the difference in binding mechanisms between PRG or 5AD and 1E9 mutants with respect to the corresponding complexes with wild type 1E9, and the difference in binding mechanisms between the PRG−1E9dm and the

PRG−DB3 complex, the individual contributions to the respective shifts, $\Delta\Delta E_{elec}$, $\Delta\Delta E_{vdW}$, and so forth, were computed. To compare the PRG−1E9dm and the PRG−DB3 complex, also the shift in the total binding free energy, $\Delta\Delta G = \Delta G_{1E9dm} - \Delta G_{DB3}$, was evaluated. For the comparison of the energetics of the PRG−1E9dm and the PRG−DB3 complex, the values for DB3 were taken from a study by Peräkylä and Nordman.[27]

The standard errors for the entropy estimates as well as for the estimation of other energetic components were determined by dividing the corresponding standard deviations by the square root of the number of configurations considered. Typical autocorrelation times of energies reside in the subpicosecond regime[53] and, hence, instantaneous energies separated by 10 ps can be considered to be statistically independent. Standard errors for energetic differences between bound and unbound states between the components for PRG−1E9dm and PRG−DB3 complexes were evaluated from the standard error from the individual values using error propagation.

3. RESULTS AND DISCUSSION

In order to understand the mechanisms underlying the binding of progesterone (PRG) and 5β-androstane-3,17-dione (5AD) to the antibody 1E9 and its variants, an energetic analysis using the MM-PB(GB)SA method was conducted. Molecular configurations obtained from MD simulations of the complexes in explicit water were used for the calculation of binding free energies. The production simulations of 10 ns carried out for these systems were stable on the basis of the total and potential energies of these systems (data not shown) and the rmsd from the X-ray structures. Here the rms deviations for the backbone atoms from the corresponding X-ray crystal structure in the simulations of PRG−1E9dm and 5AD−1E9dm are shown in Figure 3. The magnitude of atomic fluctuations of the two systems are similar. The structure of the 1E9dm−PRG complex had an average rmsd of 1.46 Å and an average rmsd of 1.56 Å was observed for the 1E9dm−5AD complex. Similar deviations have been observed earlier for similar systems.[25,27]

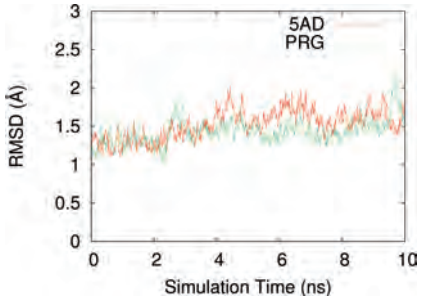

Figure 3. Variation of backbone rmsd with simulation time for the complexes PRG−1E9dm and 5AD−1E9dm.

3.1. Binding Energetics for Steroids with 1E9 and its Variants. It has been reported[17] previously that the wild-type 1E9 cross-reacts with progesterone. However, its affinity for the steroid is 10 000-fold weaker than for its cognate hapten, hexachlorobornene.[20,54] The binding mechanism of PRG and 5AD to the antibody 1E9 (wild type) and its mutant variants was discussed previously mainly based on structural aspects neglecting solvent effects.[20,21] To understand the underlying binding mechanism from an energetic perspective including solvent effects, we performed an energetic analysis of the binding of PRG and 5AD to wild type 1E9 and its variants. Here, 1000 configurations extracted from corresponding explicit water molecular dynamics simulations were analyzed using the MM-PBSA method.

3.1.1. General Contributions to Binding Affinity. The energetics of the binding of PRG and 5AD to 1E9 and its single and double mutants obtained from the MM-PBSA calculations are shown in Table 1. The mutation-induced shifts in binding free energy denoted as relative binding free energies are given in Table 2. The total binding free energies are found to range between −6 and −11.7 kcal/mol. Overall, PRG binds more strongly to 1E9 and its variants than 5AD. The weakest affinity for the steroids is observed for 1E9, and the binding affinity increases in the order Arg^{100H}Trp 1E9, Leu^{47H}Trp 1E9, and 1E9dm. In general, the largest contribution favoring binding is the van der Waals interaction between the binding partners, being in the range −40 to −44 kcal/mol for PRG and −37 to −39 kcal/mol for 5AD. The nonpolar interactions with the solvent including the contribution from the hydrophobic effect yield contributions in the range −3.6 to −3.7 kcal/mol for PRG and −3.4 to −3.6 kcal/mol for 5AD.

Association is opposed by an unfavorable desolvation of polar groups, yielding a contribution of 22.5 to 28.2 kcal/mol for PRG and 26.8 to 28.2 kcal/mol for 5AD. As found for other systems,[25−27] the unfavorable desolvation of polar groups is only partially compensated by favorable intermolecular electrostatic interactions. Intermolecular electrostatic interactions yield a contribution of −1.6 to −9.3 kcal/mol for PRG and −9.1 to −10.7 kcal/mol for 5AD. The sum of the contribution from the desolvation of polar groups and the intermolecular electrostatic interactions is 18.8 to 22.2 kcal/mol for PRG and 16.1 to 18.8 kcal/mol for 5AD.

Table 1. Free Energy Terms (kcal/mol) of 1E9 Variants for Progesterone (PRG) and 5β-Androstane-3,17-Dione (5AD)[a]

steroid	variant	ΔE_{elec}	ΔE_{vdW}	ΔG_{np}	ΔG_{pol}	ΔG_{solv}[b]	$\Delta G_{pol,elec}$[c]	$-T\Delta S_{MM}$	ΔG_{bind}
PRG	WT	−1.6(0.1)	−39.5(0.2)	−3.7(0.01)	22.5(0.2)	18.8(0.2)	20.9(0.2)	14.2(0.9)	−8.1(0.9)
	L^{47H}W	−3.5(0.03)	−44.1(0.03)	−3.8(0.01)	25.7(0.03)	21.9(0.03)	22.2(0.03)	15.5(0.8)	−10.2(0.8)
	R^{100H}W	−6.7(0.1)	−41.0(0.1)	−3.6(0.01)	27.0(0.1)	23.4(0.1)	20.3(0.1)	15.2(1.1)	−9.1(1.1)
	dm	−9.3(0.1)	−42.7(0.1)	−3.7(0.01)	28.2(0.2)	24.5(0.2)	18.9(0.2)	15.4(1.2)	−11.7(1.2)
5AD	WT	−9.4(0.2)	−36.8(0.2)	−3.5(0.01)	28.2(0.3)	24.7(0.3)	18.8(0.3)	15.5(1.1)	−6.0(1.1)
	L^{47H}W	−9.7(0.04)	−37.9(0.04)	−3.4(0.01)	28.1(0.04)	24.7(0.04)	18.4.(0.04)	14.3(0.9)	−8.2(0.9)
	R^{100H}W	−9.1(0.02)	−37.1(0.03)	−3.5(0.01)	26.1(0.03)	22.6(0.04)	17.0(0.04)	15.9(0.8)	−7.7(0.8)
	dm	−10.7(0.1)	−38.6(0.1)	−3.6(0.01)	26.8(0.1)	23.2(0.1)	16.1(0.1)	15.0(0.8)	−11.1(0.8)

[a] Standard errors of the mean are given in parentheses. Results are obtained from MM-PBSA calculations. Molecular configurations were generated using MD simulations in explicit water. [b] $\Delta G_{solv} = \Delta G_{np} + \Delta G_{pol}$. [c] $\Delta G_{pol,elec} = \Delta G_{pol} + \Delta E_{elec}$.

dx.doi.org/10.1021/jp201538t |J. Phys. Chem. B 2011, 115, 7661–7669

Table 2. Mutation-Induced Shifts in Binding Free Energy for 1E9 Mutants Complexed with Progesterone (PRG) and 5β-Androstane-3,17-Dione (5AD) from the Simulations and Previous Experiments, $\Delta\Delta G_{sim}$[b] and $\Delta\Delta G_{exp}$[c], Respectively, As Well As Mutation-Induced Increase in Binding Constants from the Simulations, r_{sim}[a]

		$\Delta\Delta G_{sim}$[b]	$\Delta\Delta G_{exp}$[b]	r_{sim}	r_{exp}[c]
steroids	variant	(kcal/mol)	(kcal/mol)	(sim)	(exp)
PRG	$L^{47H}W$	−2.1(1.2)	−2.0(0.1)	5−250	21−33
	$R^{100H}W$	−1.0(1.4)	−1.0(0.1)	1−55	4−6
	dm	−3.6(1.5)	−3.3(0.1)	33−5500	190−310
5AD	$L^{47H}W$	−2.2(1.5)	−3.0(0.1)	3−500	120−170
	$R^{100H}W$	−1.7(1.4)	−2.1(0.1)	2−180	28−42
	dm	−5.1(1.4)	−5.6(0.1)	500−60000	9700−14000

[a] Standard errors are given in parentheses. [b] $\Delta\Delta G = \Delta G_{MUT} - \Delta G_{WT}$ with ΔG_{WT} and ΔG_{MUT} taken from Table 1. [c] Obtained from eq 6 using experimental binding constants from ref 20. [d] Obtained from eq 6 replacing the subscript exp by sim.

Formation of macromolecular complexes is in general opposed by a loss in configurational entropy of the binding partners.[25,55,56] We obtain corresponding contributions to the binding of free energy of 14.2 to 15.4 kcal/mol for PRG and 14.3 to 15.9 kcal/mol for 5AD. This entropic component is often not considered in MM/PBSA calculations, partly because it may nearly cancel out in computation-induced shifts in binding free energies, which are often the main interest of such kind of studies.[51] If the entropy is at all considered, the statistical accuracy of the entropy estimates is typically not quoted and hence not included in the binding free energy. We do consider the entropic contribution and indeed find that, although the contributions to the absolute binding free energies are large, the entropic contributions largely cancel out in the relative binding free energies. However, the entropy calculation based on normal-mode analysis as used here is a memory intensive and computational expensive method; therefore, generally only 20 to 30 structures are used to estimate the entropic contribution to the binding. Although we went beyond the current state of the art using even 40 (equally spaced) configurations, we find that the standard error of the entropic contribution is an order of magnitude larger than the standard errors of the other components and is therefore limiting the statistical accuracy of the binding free energies.

Some authors reduce the computational expense of the entropy calculations by considering not the full but a truncated protein consisting of the ligand and only protein atoms at most 0.8 nm away from the ligand. In this way, a larger number of configurations can be sampled in the entropy calculations at the same computational cost. The truncation of the protein, though, can lead to conformational distortions of the fragment during energy minimization, the latter being required for the normal-mode analysis. These distortions can be avoided if a buffer region outside the truncated protein is immobilized.[50] This method was used recently by Genheden and Ryde (GR)[57] to estimate the entropic contribution to the binding free energy for a protein−ligand complex based on a 10 ns simulation of the complex as used in our study but using a sampling frequency of 1/5 ps, being a factor of 2 larger than that employed in the present work. The standard error for the binding free energies obtained by GR was 0.5 kcal/mol and, hence, indeed somewhat smaller than the standard errors of the binding free energies obtained here. GR also found that a single long simulation yields a smaller standard error than several independent short simulations.

Truncating the protein is an efficient means to improve the statistical accuracy of the entropy estimate, but it should be emphasized that this approach neglects possible long-range effects of the ligand on the structural flexibility of distal regions in the protein. For example, the molecular motor kinesin which acts as an enzyme for hydrolysis of adenosintriphosphate exhibits a domain denoted as neck linker that is 3 nm away from the nucleotide binding pocket but whose flexibility (and, hence, configurational entropy) strongly depends on the ligand.[58] Whether or not such allosteric effects exist for a given system may not be known a priori.

3.1.1a. Binding of 5AD to 1E9 versus PRG to 1E9. The binding affinity of 5AD to 1E9 is lower than that of PRG to 1E9, indicated by a positive shift in binding free energy of +2.1 kcal/mol. The desolvation of polar groups and the intermolecular electrostatic interactions for 5AD binding to 1E9 is more favorable than the corresponding contributions to the binding of 5AD to 1E9 ($\Delta\Delta G_{pol,elec} = -2.1$ kcal/mol). However, the intermolecular van der Waals interactions between 5AD and 1E9 are weaker than those between PRG and 1E9 ($\Delta\Delta E_{vdW} = +2.7$ kcal/mol). The nonpolar solvation free energy is marginally less favorable ($\Delta\Delta G_{np} = +0.2$ kcal/mol) for the binding of 5AD to 1E9 than for the binding of PRG to 1E9.

3.1.2. Mutation-Induced Increase in Binding Affinity. The mutation-induced increase in binding affinity may be inferred from the corresponding shift in the binding free energy for the 1E9 mutants relative to the binding free energy of wild type 1E9, this shift being denoted as relative binding free energy. The relative binding affinities are summarized in Table 2, which also gives the corresponding experimental values. Unfortunately, the statistical error for the relative binding free energies is of the same order of magnitude as the relative binding free energies themselves. Nevertheless, the relative binding free energies from the simulations show the same ranking as those from the experiments, although the free energy shifts of the single mutants have low statistical significance. Nevertheless, significant shifts in binding free energies are observed for the double mutant; the relative binding free energies of PRG−1E9dm and 5AD−1E9dm are −3.6 ± 1.5 and −5.1 ± 1.4 kcal/mol, respectively, which is in agreement with the experimental values.

The mechanism underlying the mutation-induced changes in affinity may be elucidated from the variation of different components of the binding free energy upon mutations that can be deduced from Table 1. The relative binding free energy of PRG to 1E9dm is −3.6 kcal/mol, corresponding to an increase in affinity. This increase in affinity correlates with favorable shifts in (i) the van der Waals interactions by −3.2 kcal/mol and (ii) the contribution from polar interactions within the binding partners and with the solvent by −2 kcal/mol. The change from in the desolvation of nonpolar groups is zero. The contribution from the change in entropy of the binding partners is slightly shifted by +1.2 kcal/mol, thus being more unfavorable for 1E9dm than for 1E9.

The relative binding free energy for the 5AD−1E9dm complex is −5.1 kcal/mol. The increased binding affinity for 5AD −1E9dm correlates with a favorable shift in the intermolecular van der Waals interactions by −1.3 kcal/mol, a slightly enhanced desolvation of nonpolar groups yielding a contribution

of −0.1 kcal/mol, and more favorable electrostatics yielding a contribution of −2.7 kcal/mol.

The binding free energies of the 5AD−1E9dm complex and the PRG−1E9dm complex are the same within the error. Comparing the 5AD−1E9dm complex with the PRG−1E9dm complex, however, reveals differences in the binding mechanisms that can be related to the experimental structures. We find that the van der Waals interactions are more favorable for the PRG−1E9dm complex than for the 5AD−1E9dm complex, amounting to −42.7 versus −38.6 kcal/mol. This correlates well with a higher number of intermolecular van der Waals contacts for PRG−1E9dm (46) compared to 5AD−1E9dm (42).[21] Normalizing the van der Waals energy by the number of van der Waals contacts yields −0.929 kcal/mol for PRG−1E9dm and −0.919 for 5AD−1E9dm. Hence, the van der Waals energy is found to scale linearly with the number of van der Waals contacts with an average energy of −0.92 to −0.93 kcal/mol per contact. This is close to the usual van der Waals energies ranging from −0.1 and −0.8 kcal/mol per contact.[59] The somewhat larger magnitude found here may arise from the fact that not only immediate contacts but also more long-range interactions contribute to the van der Waals energies. The larger number of van der Waals contacts that 1E9dm forms with PRG compared to 5AD also implies a somewhat better shielding of nonpolar groups from the solvent, which is reflected in the contribution from the nonpolar solvation which is −0.1 kcal/mol more favorable for PRG than for 5AD.

On the other hand, both the electrostatic interactions between the protein and the ligand and the polar contribution to the solvation free energy are more favorable for 5AD−1E9dm than for PRG−1E9dm, together contributing −2.8 kcal/mol to the shift in binding free energy. Similarly, comparing the decomposition of the binding free energies of 5AD−DB3 and PRG−DB3[27] showed that the van der Waals components favor binding of PRG, whereas the polar solvation free energies favor binding of 5AD to DB3. In contrast to the corresponding steroid−1E9dm complexes, the intermolecular electrostatic interactions are more favorable for PRG−DB3 than for 5AD−DB3.

To summarize, the increased affinity of both steroids to 1E9dm compared to 1E9 is due to increased intermolecular van der Waals interactions and more favorable total electrostatic interactions. For 5AD, the total electrostatic interactions provide even the dominant contribution to the increase in binding affinity. Whereas the role of van der Waals interactions was suggested based on the X-ray structures of the complexes, the role of the total electrostatic interactions was not anticipated previously.

3.2. Interactions Governing Binding of PRG to 1E9dm versus DB3. Inspection of the X-ray structures suggested that the mechanisms by which PRG is bound by 1E9dm and DB3 are different; whereas strong hydrogen bonds between the receptor and the ligands exist in the case of DB3, 1E9dm does not form hydrogen bonds with the steroids. Verdino et al. claimed that the lack of hydrogen bonding interactions for the PRG−1E9dm complex is compensated by the deeper penetration of 1E9 by the steroids and the resulting increase in the number of van der Waals contacts.[21] However, in fact in the X-ray structures PRG forms even less van der Waals contacts with 1E9dm (46) than with DB3 (59),[12,21] so the mechanism proposed by Verdino et al. cannot apply. To understand the difference in binding mechanisms between PRG−1E9dm and PRG−DB3, we have calculated the shift of binding free energies and their individual components for PRG−1E9dm with respect to PRG−DB3, by comparing our results for 1E9dm and the results from a study for DB3 by Peräkylä and Nordman,[27] as shown in Table 3.

Table 3. Free Energy Terms of PRG−1E9dm Relative to PRG−DB3 Complex[a,b] in kcal/mol[c]

component	value
$\Delta\Delta E_{elec}$	+8.2(0.3)
$\Delta\Delta E_{vdW}$	+4.8(0.3)
$\Delta\Delta G_{np}$	+1.0(0.01)
$\Delta\Delta G_{pol}$	−13.1(0.3)
$\Delta\Delta G_{solv}$	−12.1(0.4)
$\Delta\Delta G_{pol,elec}$	−4.9(0.4)
$\Delta\Delta G_{bind}$	+1.3(0.2)

[a] $\Delta\Delta G = \Delta G^{1E9dm} - \Delta G^{DB3}$ [b] Free energy terms for the PRG−DB3 complex were obtained from ref 27. [c] Standard errors of the mean are given in parentheses.

It should be mentioned that there are slight deviations in the simulation protocols between the current and the previous study. In particular, the time scales used for the MD trajectories considered by Peräkylä and Nordman were more than an order of magnitude shorter than the ones used in the current investigation (0.5 instead of 10 ns). Furthermore, Peräkylä and Nordman did not compute the entropic component of the binding free energy. Hence, in order to compare our results with those for DB3, we consider the binding free energies for 1E9dm without the component from the entropy of the binding partners. Table 1 shows that this entropic component is barely affected by mutations, so it is expected to largely cancel out in the difference in binding free energies. Finally Peräkylä and Nordman did not provide standard errors but standard deviations that highly overestimate the statistical error. In order to have improved estimates for the statistical accuracy of their results, we computed the corresponding standard errors from their standard deviations.

The PRG−1E9dm complex has a somewhat lower affinity than the PRG−DB3 complex; the corresponding shift in binding free energy of +1.3 kcal/mol is in agreement with the experimental value of +1 kcal/mol. The polar protein−ligand interactions are less favorable for PRG−1E9dm than for PRG−DB3 by +8.2 kcal/mol. This correlates well with a lack of hydrogen bonds between PRG and 1E9dm and the existence of two hydrogen bonds between PRG and DB3. On the other hand, the contribution from the desolvation of polar groups is less unfavorable for PRG−1E9dm than for PRG−DB3 by −13.1 kcal/mol. In line with this observation, the X-ray structures show that one of PRG's two carbonyl groups is buried in the binding pocket for both complexes and the other carbonyl group is strongly solvent exposed for PRG−1E9dm but barely exposed for PRG−DB3. The net contribution from polar interactions to the binding free energy is more favorable for PRG−1E9dm than for PRG−DB3 by −4.9 kcal/mol.

PRG shows weaker van der Waals interactions with 1E9dm than with DB3 (shift of +4.8 kcal/mol). This correlates well with the decreased number of van der Waals contacts between PRG and 1E9dm (46) compared to PRG and DB3 (59). Interestingly, the van der Waals energy per contact is slightly higher in magnitude for PRG/1E9dm (−0.9 kcal/mol) than for PRG/DB3 (−0.8 kcal/mol), possibly indicating better optimization

and less frustration of individual contacts when less contacts are formed. The decreased number of van der Waals contacts between PRG and 1E9dm correlates with increased unfavorable nonpolar interactions between the solutes and the solvent, yielding a contribution of +1 kcal/mol.

Altogether, for PRG−1E9dm the solutes remain more strongly exposed to the solvent than for PRG−DB3. On the one hand, this leads to weaker van der Waals interactions between the binding partners and increased unfavorable nonpolar contributions to the binding free energy, stabilizing PRG−DB3 over PRG−1E9dm. On the other hand, the stronger solvation of polar groups stabilizes the PRG−1E9dm over the PRG−DB3 complex. Both effects largely balance each other such that the net difference in affinity between the two complexes is small.

4. SUMMARY AND CONCLUSION

We have studied the binding of two structurally distinct steroids, progesterone and 5β-androstane-3,17-dione, to the antibody 1E9, its double mutant 1E9dm, and the corresponding single mutants, using a combination of molecular mechanical energies derived from MD simulations in explicit water, solvation free energies derived from the PBSA solvation model, and the solute entropy contributions derived from normal-mode analysis. Mutation-induced changes in affinity are in good agreement with experiment. Among the variants studied, 1E9 exhibits the lowest affinity for the steroids. The $Leu^{H47}Trp/Arg^{100H}Trp$ substituted double mutant 1E9dm almost fully mimics the properties of DB3 with respect to the ligand binding affinity. Because of the double mutations, the shape of the 1E9 binding pocket is significantly altered and the resultant combining binding site of the 1E9dm now resembles a fusion between wild type 1E9 and DB3 (see Figure 2). Protein−steroid complex formation is favored by the van der Waals interactions, the electrostatic component of the molecular mechanical energy and the nonpolar component of the solvation free energy. In all cases, the most important favorable term favoring complex formations is provided by the van der Waals energy, whereas the total contribution from the intermolecular electrostatic interactions and the desolvation of polar groups is unfavorable, both in agreement with earlier studies of other systems.[25,27]

Comparing the factors governing the binding of PRG and that of 5AD to 1E9dm shows that similar affinities arise from different underlying mechanisms. On the one hand, the binding of PRG to 1E9dm is favored by stronger van der Waals interactions than present for the 5AD−1E9dm complex. This correlates with a higher number of van der Waals contacts present for PRG−1E9dm compared to 5AD−1E9dm. On the other hand, both the electrostatic interactions between the protein and the ligand and the polar contribution to the solvation free energy are more favorable for 5AD−1E9dm than for PRG−1E9dm. Similarly, comparing the decomposition of the binding free energies of 5AD−DB3 and PRG−DB3 showed that the van der Waals components favor binding of PRG, whereas the polar solvation free energies favor binding of 5AD to DB3.[27]

PRG−1E9dm shows weaker intermolecular electrostatic interactions than PRG−DB3, correlating with the observation that PRG forms no hydrogen bond with 1E9dm but two hydrogen bonds with DB3. PRG also exhibits weaker van der Waals interactions with 1E9dm than with DB3 and a larger unfavorable contribution from the nonpolar solvation free energy. This is contrasting the claim by Verdino et al. that PRG penetrates more deeply into the binding pocket of 1E9dm than into that of DB3. However, the observed trend in the van der Waals energies is consistent with the lower number of van der Waals contacts between PRG and 1E9dm (46) than between PRG and DB3 (59).[21,27] On the other hand, PRG−1E9dm is stabilized by a stronger solvation of polar groups.

Altogether, though the complexes formed by PRG or 5AD with 1E9dm and by PRG with DB3 have similar affinity, the binding mechanisms are different. Decreased van der Waals interactions observed for 5AD−1E9dm versus PRG−1E9dm or for PRG−1E9dm versus PRG−DB3 are energetically compensated by an increased solvation of polar groups. This work illustrates that deducing binding mechanisms from structural models of the binding partners alone can be misleading. In contrast, taking into account solvation effects as done in MM-PBSA calculations is essential to understand molecular recognition.

■ ASSOCIATED CONTENT

Supporting Information. Structures of the combining sites of $L^{H47}W$ 1E9 and $R^{H100}W$ 1E9 with bound PRG, as well as free energy calculations for binding of PRG and 5AD to 1E9 and its variants using more efficient but more approximate methods. This material is available free of charge via the Internet at http://pubs.acs.org.

■ AUTHOR INFORMATION

Corresponding Author

*E-Mail: Volker.Knecht@mpikg.mpg.de. Phone: +49-331-5679732. Fax: +49-331-5679612.

■ ACKNOWLEDGMENT

The work was supported by Federal Ministry of Education and Research (BMBF), Germany.

■ REFERENCES

(1) Liu, D. R.; Schultz, P. G. *Angew. Chem., Int. Ed.* **1999**, *38*, 36–54.
(2) Dill, K. A. *Biochemistry* **1990**, *29*, 7133–7155.
(3) Koh, J. T. *Chem. Biol.* **2002**, *9*, 17–23.
(4) Arevalo, J. H.; Hassig, C. A.; Stura, E. A.; Sims, M. J.; Taussig, M. J.; Wilson, I. A. *J. Mol. Biol.* **1994**, *241*, 663–690.
(5) Wilson, I. A.; Stanfield, R. L. *Curr. Opin. Struct. Biol.* **1994**, *4*, 857–867.
(6) Charbonnier, J. B.; Golinelli-Pimpaneau, B.; Gigant, B.; Tawfik, D. S.; Chap, R.; Schindler, D. G.; Kim, S. H.; Green, B. S.; Eshhar, Z.; Knossow, M. *Science* **1997**, *275*, 1140–1142.
(7) Gigant, B.; Charbonnier, J. B.; Eshhar, Z.; Green, B. S.; Knossow, M. *Proc. Nat. Acad. Sci. U.S.A.* **1997**, *94*, 7857–7861.
(8) Wedemayer, G. J.; Patten, P. A.; Wang, L. H.; Schultz, P. G.; Stevens, R. C. *Science* **1997**, *276*, 1665–1669.
(9) Jeffrey, P. D.; Strong, R. K.; Sieker, L. C.; Chang, C. Y. Y.; Campbell, R. L.; Petsko, G. A.; Haber, E.; Margolies, M. N.; Sheriff, S. *Proc. Natl. Acad. Sci. U.S.A.* **1993**, *90*, 10310–10314.
(10) Trinh, C. H.; Hemmington, S. D.; Verhoeyen, M. E.; Phillips, S. E. V. *Science* **1997**, *7*, 937–948.
(11) Arevalo, J. H.; Stura, E. A.; Taussig, M. J.; Wilson, I. A. *J. Mol. Biol.* **1993**, *231*, 103–118.
(12) Arevalo, J. H.; Taussig, M. J.; Wilson, I. A. *Nature* **1993**, *365*, 859–863.

(13) Hilvert, D.; Hill, K. W.; Nared, K. D.; Auditor, M-T. M. *J. Am. Chem. Soc.* **1989**, *111*, 9261–9262.
(14) Pindur, U.; Lutz, G.; Otto, C. *Chem. Rev.* **1993**, *93*, 741–761.
(15) Laschat, S. *Angew. Chem., Int. Ed. Engl.* **1996**, *35*, 289–291.
(16) Piatesi, A.; Hilvert, D. *ChemBioChem.* **2004**, *5*, 460–466.
(17) Haynes, M. R.; Lenz, M.; Taussig, M. J.; Wilson, I. A.; Hilvert, D. *Isr. J. Chem.* **1996**, *36*, 151–159.
(18) Xu, J.; Deng, Q.; Chen, J.; Houk, K. N.; Bartek, J.; Hilvert, D.; Wilson, I. A. *Science* **1999**, *286*, 2345–2348.
(19) Chen, J.; Deng, Q.; Wang, R.; Houk, K. N.; Hilvert, D. *ChemBioChem* **2000**, *1*, 255–261.
(20) Piatesi, A.; Aldag, C.; Hilvert, D. *J. Mol. Biol.* **2008**, *377*, 993–1001.
(21) Verdino, P.; Aldag, C.; Hilvert, D.; Wilson, I. A. *Proc. Natl. Acad. Sci. U.S.A.* **2008**, *105*, 11725–11730.
(22) Mills, N. *J. Am. Chem. Soc.* **2006**, *128*, 13649–13650.
(23) Pattersen, E. F.; Goddard, T. D.; Huang, C. C.; Couch, G. S.; Greenblatt, D. M.; Meng, E. C.; Ferrin, T. E. *J. Comput. Chem.* **2004**, *25*, 1605–1612.
(24) Kubinyi, H. Hydrogen Bonding: The Last Mystery in Drug Design? In *Pharmacokinetic Optimization in Drug Research: Biological, Physiochemical, and Computational Strategies*; Testa, B., van de Waterbeemd, H.; Folkers, G., Guy, R., Eds.; Verlag Helvetica Chimica Acta: Zürich, 2007; pp 513−524.
(25) Chong, L. T.; Duan, Y.; Wang, L.; Massova, I.; Kollman, P. A. *Proc. Natl. Acad. Sci. U.S.A.* **1999**, *96*, 14330–14335.
(26) Kuhn, B.; Kollman, P. A. *J. Med. Chem.* **2000**, *43*, 3786–3791.
(27) Peräkylä, M.; Nordman, N. *Protein Eng.* **2001**, *14*, 753–758.
(28) Kollman, P. A. *Chem. Rev.* **1993**, *93*, 2395–2417.
(29) Lybrand, T.; McCammon, J. A.; Wipff, G. *Proc. Natl. Acad. Sci. U.S.A.* **1986**, *83*, 833–835.
(30) Jayaram, B.; Sprous, D.; Young, M. A.; Beveridge, D. L. *J. Am. Chem. Soc.* **1998**, *120*, 10629–10633.
(31) Vorobjev, Y. N.; Almagro, J. C.; Hermans, J. *Proteins* **1998**, *32*, 399–413.
(32) Kollman, P. A.; Massova, I.; Reyes, C.; Kuhn, B.; Huo, S.; Chong, L.; Lee, M.; Lee, T.; Duan, Y.; Wang, W.; Donini, O.; Cieplak, P.; Srinivasan, J.; Case, D. A.; Cheatham, T. E. *Acc. Chem. Res.* **2000**, *33*, 889–897.
(33) Rastelli, G.; Rio, A. D.; Degliesposti, G.; Sgobba, M. *J. Comput. Chem.* **2010**, *31*, 797–810.
(34) Reyes, C. M.; Kollman, P. A. *J. Mol. Biol.* **2000**, *295*, 1–6.
(35) Reyes, C. M.; Kollman, P. A. *J. Mol. Biol.* **2000**, *297*, 1145–1158.
(36) Nordman, N.; Valjakka, J.; Peräkylä, M. *Proteins: Struct., Funct., Genet.* **2003**, *50*, 135–143.
(37) Karplus, M.; Kushick, J. N. *Macromolecules* **1981**, *14*, 325–332.
(38) Rempe, S. B.; Jonsson, H. *Chem. Educ.* **1998**, *3*, 1–17.
(39) Hornak, V.; Abel, R.; Okur, A.; Strockbine, B.; Roitberg, A.; Simmerling, C. *Proteins* **2006**, *65*, 712–725.
(40) Wang, J.; Wolf, R. M.; Caldwell, J. W.; Kollman, P. A.; Case, D. A. *J. Comput. Chem.* **2004**, *25*, 1157–1174.
(41) Jakalian, A.; Jack, D. B.; Bayly, C. I. *J. Comput. Chem.* **2002**, *23*, 1623–1641.
(42) Wang, J.; Wang, W.; Kollman, P. A.; Case, D. A. *J. Mol. Graphics Model.* **2006**, *25*, 247–260.
(43) Case, D. A.; Cheatham, T. E.; Darden, T.; Gohlke, H.; Luo, R.; Merz, K. M.; Onufriev, A.; Simmerling, C.; Wang, B.; Woods, R. *J. Computat. Chem.* **2005**, *26*, 1668–1688.
(44) Dewar, M. J. S.; Zoebisch, E. G.; Healy, E. F.; Stewart, J. J. P. *J. Am. Chem. Soc.* **1985**, *107*, 3902–3909.
(45) Jorgensen, W. L.; Chandrasekar, J.; Madura, J. D.; Impey, R.; Klein, K. *J. Chem. Phys.* **1983**, *79*, 926–935.
(46) Ryckaert, J.-P.; Ciccotti, G.; Berendsen, H. J. C. *J. Comput. Phys.* **1977**, *23*, 327–341.
(47) Darden, T.; York, D.; L. Pedersen, L. *J. Chem. Phys.* **1993**, *98*, 10089–10092.
(48) Sitkoff, D.; Sharp, K. A.; Honig, B. *J. Phys. Chem.* **1994**, *98*, 1978–1988.
(49) Swanson, J. M.; Henchman, R. H.; McCammon, J. A. *Biophys. J.* **2004**, *86*, 67–74.
(50) Kongsted, J.; Ryde, U. *J. Comput.-Aided Mol. Des.* **2009**, *23*, 63–71.
(51) Massova, I.; Kollman, P. A. *J. Am. Chem. Soc.* **1999**, *36*, 8133–8143.
(52) Baker, N.; Sept, D.; Joseph, S.; Holst, M.; J. McCammon, J. *Proc. Natl. Acad. Sci. U.S.A.* **1998**, *98*, 10037–10041.
(53) Kittner, M.; Knecht, V. *J. Phys. Chem. B* **2010**, *114*, 15288–15295.
(54) Davies, D. R.; Padlan, E. A.; Sheriff, S. *Annu. Rev. Biochem.* **1990**, *59*, 439–473.
(55) Gilson, M. K.; Zhou, H. X. *Annu. Rev. Biophys. Biomol. Struct.* **2007**, *36*, 21–42.
(56) Knecht, V. *J. Phys. Chem. B* **2010**, *114*, 12701–12707.
(57) Genheden, S.; Ryde, U. *J. Comput. Chem.* **2010**, *31*, 837–846.
(58) Rice, S.; Lin, A. W.; Safer, D.; Hart, C. L.; Naber, N.; Carragher, B. O.; Cain, S. M.; Pechatnikova, E.; Wilson-Kubalek, E. M.; Whittaker, M.; Pate, E.; Cooke, R.; Taylor, E. W.; Milligan, R. A.; Vale, R. D. *Nature* **1999**, *402*, 778–784.
(59) Garrett, R.; Grisham, C. M. *Biochemistry*, 4th ed.; Brooks Cole Publishing: CA, 2008; p 12.